ELSEVIER

Journal of Alloys and Compounds 323–324 (2001) 654–660

Journal of ALLOYS AND COMPOUNDS

www.elsevier.com/locate/jallcom

Experimental and theoretical study of ligand field, 4f–4f intensities and emission quantum yield in the compound $Eu(bpyO_2)_4(ClO_4)_3$

O.L. Malta[a,*], J. Legendziewicz[b], E. Huskowska[b], I. Turowska-Tyrk[c], R.Q. Albuquerque[a], C. de Mello Donegá[a], F.R.G. e Silva[a]

[a]*Departamento de Química Fundamental-CCEN-UFPE-Cidade Universitária, Recife-PE, 50670-901, Brazil*
[b]*Faculty of Chemistry, University of Wrocław, Joliot-Curie 14, 50-383, Wrocław, Poland*
[c]*Institute of Physical and Theoretical Chemistry, Wrocław University of Technology, Wybrzeze Wyspianskiego 27, 50-370, Wrocław, Poland*

Abstract

The high resolution emission spectrum of the Eu^{3+} ion in the compound $Eu(bpyO_2)_4(ClO_4)_3$, where $bpyO_2$=2,2′-bipyridine-1,1′-dioxide, has been previously studied in solid state and frozen solution. The compound crystallizes in the monoclinic $P2_1$ space group with the cell parameters a=14.730(1) Å, b=13.585(1) Å, c=22.967(2) Å and β=91.46(1)°. The coordination polyhedron can be described as a distorted cube into a square antiprism with symmetry close to D_2. The experimental emission quantum yield (q) was measured according to a method previously described and a q-value of 15% was obtained. By using the structural crystallographic data a theoretical ligand field and intensity analysis was carried out, and the sparkle model was applied to obtain the electronic structure of the organic part of the compound. From these results, intramolecular energy transfer rates were evaluated according to a recently developed model. An appropriate set of rate equations for the normalized populations of the levels involved was solved numerically, by using the 4th order Runge–Kutta method, and a theoretical q-value could be obtained (19.6%), which is in good agreement with experiment. A relevant aspect is that the reason for this rather low q-value could be explained in terms of the relative position of the lowest ligand triplet energy level with respect to the $^5D_1$ and $^5D_0$ levels of the Eu^{3+} ion. The theoretical analysis has also shown that, in this compound, a slight decrease in the energy of the ligand triplet level is sufficient to quench almost completely the Eu^{3+} luminescence.

Keywords: Lanthanide complexes; Spectroscopy; Quantum yield

1. Introduction

Much effort has been devoted to the design of new luminescent lanthanide complexes suitable as agents which have the potential to bind selectively and are strongly luminescent as a result of an efficient energy transfer process from the $\pi\pi^*$ ligand excited states to 4f excited states of the lanthanide ion. The efficiency of this process is controlled by several factors and has been the subject of both experimental and theoretical investigations [1]. Recently, spectroscopy, photophysics and dynamics of excited states of europium complex with $bpyO_2$ [2] and two classes of lanthanide cryptates bearing biisoquinoline dioxide ($biqO_2$) [3,4] and bpy and $biqO_2$ units [5] have been reported. It has been found by Prodi et al. [5] and by some of us [4] that both ligand-to-metal charge transfer (LMCT) states and ligand $^3\pi\pi^*$ states controlled the energy transfer processes in both types of cryptates.

In the present work we report on the results of X-ray diffraction and 4f–4f emission quantum yield (experimental and theoretical) for the compound $Eu(bpyO_2)_4(ClO_4)_3$, where $bpyO_2$=2,2′-bipyridine-1,1′-dioxide, focusing on the investigation of the parameters governing the rather low quantum yield (15%) observed in this compound. The theoretical description of the emission quantum yield is based on a theoretical scheme that gathers the results from the sparkle model for the calculation of lanthanide complexes [6], implemented in the program MOPAC93, and a model of intramolecular energy transfer in coordination compounds [7,8]. Both models require the crystallographic data as input. This scheme has proven to be useful in the assignment of intramolecular energy transfer channels and mechanisms, and in the identification of parameters governing the emission quantum yields [1]. The theoretical analysis shows that this rather low emission quantum yield value can be explained in terms of the energetic resonance

*Corresponding author. Tel.: +55-81-271-8441; fax: +55-81-271-8442.

E-mail address: omlm@npd.ufpe.br (O.L. Malta).

0925-8388/01/$ – see front matter
PII: S0925-8388(01)01027-1

condition between the lowest ligand triplet level and the $^5D_1$ and $^5D_0$ levels of the Eu^{3+} ion. It also indicates that, in the present case, there is no influence of LMCT states, contrary to the case of macrocyclic ligands and in agreement with the fact that in the spectral region studied here no LMCT state could be detected.

2. Experimental

2.1. X-ray diffraction results

Single crystals of $Eu(bpyO_2)_4(ClO_4)_3$ of formulae $C_{40}H_{32}Cl_3EuN_8O_{20}$ were obtained from CH_3CN or from water solutions [2,9]. The kind of solvent influences the packing of the molecules in the structure so that the crystals obtained from acetonitrile are much more stable. However, crystals growing up from both types of solvents are not of very good quality, which affects the results of X-ray diffraction. The temperature of the diffraction measurements varied from 4 K to 293 K. The measurements were made in a Kuma KM4CCD diffractometer equipped with a CCD camera. Precise cell constants were determined by the least-squares method on the grounds of most of the data collection reflections. 23,707 reflections were collected, of which 11,766 were unique and 9,802 unique observed. The data were corrected for the Lorentz polarization effect [10]. The structure was solved by Patterson techniques from the SHELXS86 program [11]. Positions of only a part of non-hydrogen atoms were revealed, the remaining atoms were found by many difference Fourier syntheses. The structure was refined by the SHELXL93 program [12]. All non-hydrogen atoms were treated anisotropically. Hydrogen atoms were found geometrically and were refined with constraints. The perchlorate anions are disordered in the crystal lattice and in one of them an oxygen atom was not localized. In the refinement process many restraints were applied, but a part of them was released in the final stages of the structure determination. The final conventional *R*-value was 0.119.

The compound crystallizes in the monoclinic $P2_1$ space group with $Z=4$. The unit cell constants are $a=14.730(1)$ Å, $b=13.585(1)$ Å, $c=22.967(2)$ Å and $\beta=91.46(1)°$. The Eu^{3+} ion forms an eight-coordinated complex with bipyridine dioxide in a similar way as the lanthanum compound reported earlier [13]. In contrast to the structure of the lanthanum compound, Eu^{3+} ions are not equivalent and occupy two positions, Eu(1) and Eu(2), with somewhat different M–O distances. Moreover, Eu(1)–O(1a) and Eu(1)–O(2a) bond lengths with the same $bpyO_2$ molecule differ meaningly, whereas in the lanthanum complex they are the same. All M–O bond lengths are shorter than the respective La–O bonds and longer than the respective europium bonds with $bpyO_2$ and $biqO_2$ units in cryptates [4,14].

The resultant structure, only for the Eu(1) site, is depicted in Fig. 1. The complex can create two isomers. Selected fractional atomic coordinates which were used in the calculations are given in Table 1. The europium complex with $bpyO_2$ create polyhedra which can be described as intermediate between a square antiprism and a dodecahedron with point symmetry close to D_2. The data indicate a deformation of the almost perfect cube in the $La(bpyO_2)_4(ClO_4)_3$ complex [13] and also the effect of decrease of ionic radius of the Eu^{3+} ion on the formation of the crystal structure. The angles between two pyridine

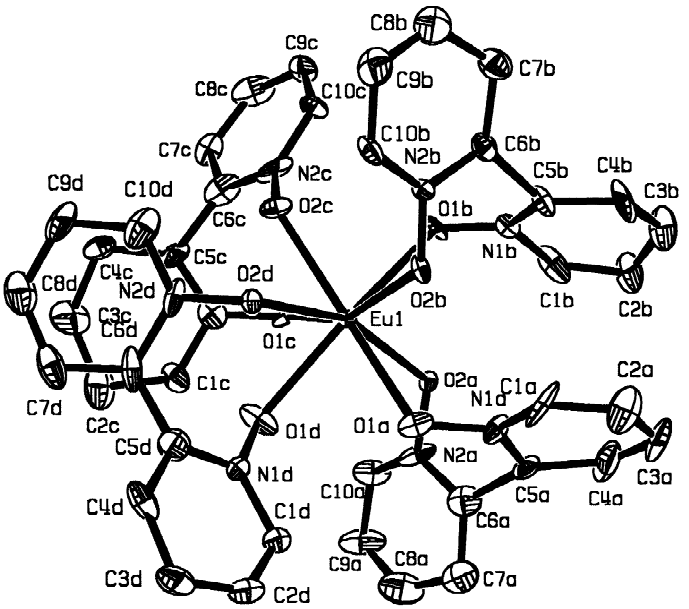

Fig. 1. An Ortep view of the Eu(1) complex with the atomic labels. The thermal ellipsoids were drawn on the 20% probability. Hydrogen atoms were omitted for clarity.

Table 1
Fractional atomic coordinates and equivalent isotropic displacement parameters (Å^2) for selected atoms of the coordination sphere. U_{eq} is defined as one third of the trace of the orthogonalized U_{ij} tensor

	x	y	z
Eu(1)	0.75131(4)	0.00207(7)	0.03750(3)
O(1a)	0.7203(11)	0.1360(15)	−0.0312(8)
O(2a)	0.8824(8)	0.0227(10)	−0.0227(5)
O(1b)	0.7698(12)	−0.1488(12)	−0.0133(7)
O(2b)	0.6159(7)	−0.0301(11)	−0.0202(6)
O(1c)	0.8858(8)	−0.0336(11)	0.0978(6)
O(2c)	0.7240(10)	−0.1223(13)	0.1057(8)
O(1d)	0.7838(10)	0.1456(14)	0.0900(10)
O(2d)	0.6194(9)	0.0472(12)	0.0956(6)
Eu(2)	0.25246(12)	0.0055(2)	0.46220(5)
O(1e)	0.1158(16)	0.0255(15)	0.4005(8)
O(2e)	0.2718(14)	0.1275(14)	0.3906(7)
O(1f)	0.3849(17)	−0.0438(18)	0.4075(8)
O(2f)	0.2213(14)	−0.1410(13)	0.4117(7)
O(1g)	0.3831(14)	0.0563(18)	0.5161(10)
O(2g)	0.2277(11)	0.1659(17)	0.5101(7)
O(1h)	0.2713(13)	−0.1149(17)	0.5337(7)
O(2h)	0.1244(13)	0.0056(22)	0.5226(11)

planes in the bipyridine molecules in the complex are in the range 57.9–68.5° and 55.3–65.9° for the Eu(1) and Eu(2), respectively, and are more opened than in the cryptands containing this type of *N*-oxide groups [4,14]. These angles are influenced by steric constraints.

2.2. Spectral measurements

The luminescence spectrum of the $Lu(bpyO_2)_4(ClO_4)_3$ complex was obtained by scanning a 1 m double-grating Jobin–Yvon U-1000 monochromator. The excitation wavelength was selected by a 0.25 m Jobin–Yvon H-10 monochromator, using a 150 W Xe lamp as the excitation source. The light detection was performed by a water-cooled RCA C31034 photomultiplier tube, the photocurrent signal being acquired through a EG&G discriminator model 1182 and digitally stored by a Jobin–Yvon Spectralink interface and a personal computer. The powder sample was kept in a quartz Dewar flask at liquid nitrogen temperature (77 K).

The excitation and emission spectra of the $Eu(bpyO_2)_4(ClO_4)_3$ complex were obtained by using a SPEX DM3000F Spectrofluorometer with double-grating 0.22 m SPEX 1680 monochromators, and a 450 W Xe Lamp as the excitation source. This set-up is equipped with an Oxford LF205 liquid Helium flow cryostat, allowing for measurements down to 4.2 K. The spectra are corrected for the instrumental response.

Excited state decay-time measurements were performed at 298 and 77 K using the 3rd harmonic of a Nd–YAG laser (10 Hz) as the excitation source. The emission was detected with a modified 1P28 photomultiplier tube, after dispersion through a 0.25 m monochromator. A filter was used to cut-off any residual laser light. The signal was then analyzed on a boxcar. The temporal resolution of the overall system is ca. 50 ns.

The emission quantum yield q is defined as the ratio between the number of photons emitted by the Eu^{3+} ion and the number of photons absorbed by the ligand. The q-value for a given sample can be determined following a method which has been described in detail elsewhere [1]:

$$q_x = \left(\frac{1-r_{ST}}{1-r_x}\right)\left(\frac{\Delta\Phi_x}{\Delta\Phi_{ST}}\right) q_{ST} \quad (1)$$

where r_{ST} and r_x are the reflectance of a standard phosphor and of the sample, respectively, and q_{ST} is the quantum yield of the standard phosphor. The terms $\Delta\Phi_x$ and $\Delta\Phi_{ST}$ give the integrated photon flux (photons. s^{-1}) for the sample and the standard phosphor, respectively. The values of r_{ST}, r_x, $\Delta\Phi_x$ and $\Delta\Phi_{ST}$ were obtained for the same excitation wavelength, geometry, powder layer thickness (2 mm) and instrumental conditions. The quantum yield standard was sodium salicylate (Merck P.A.), which has a broad band emission with a maximum at 450 nm and $q = 60\%$ at room temperature [1]. The reflection coefficients r were established by using MgO as a reflectance standard ($r = 0.91$ [1]). Three measurements were carried out for each sample. The method is accurate within 10%.

The emission spectrum of $Lu(bpyO_2)_4(ClO_4)_3$ at 77 K is shown in Fig. 2, and consists of a broad band, peaked at 545 nm, ascribed to a ligand transition from the lowest triplet state. The decay time of this emission is 2 μs at 77 K. At room temperature the emission is completely quenched.

Fig. 3 presents the emission spectrum of $Eu(bpyO_2)_4(ClO_4)_3$ at 4.2 K. The emission lines can be ascribed to the $^5D_0 \rightarrow {}^7F_J$ (J = 0–4) transitions of the Eu^{3+} ion. Very weak $^5D_1 \rightarrow {}^7F_J$ emission lines can also be observed. In contrast with the $Lu(bpyO_2)_4(ClO_4)_3$ complex, the ligand emission is no longer observable. The emission spectrum at room temperature is essentially

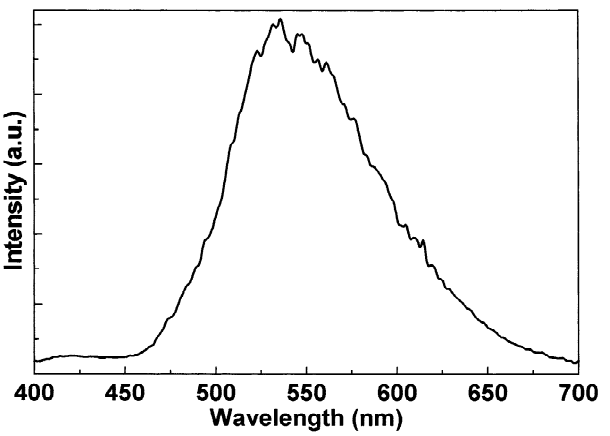

Fig. 2. The emission spectrum of $Lu(bpyO_2)_4(ClO_4)_3$ at 77 K upon 360 nm excitation.

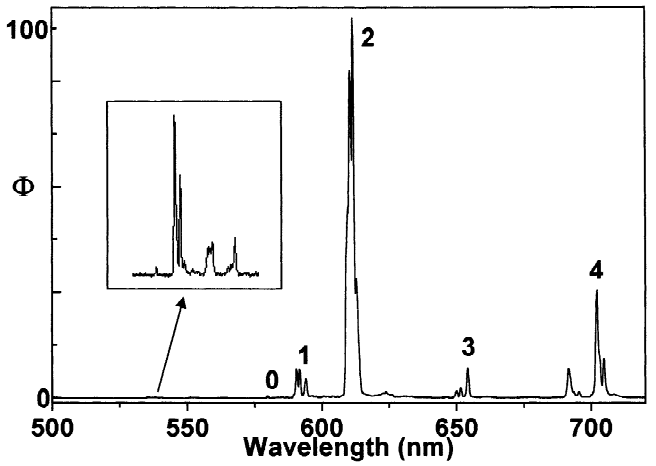

Fig. 3. The emission spectrum of $Eu(bpyO_2)_4(ClO_4)_3$ at 4.2 K, upon ligand excitation (310 nm). Φ gives the radiant power per constant wavelength interval in arbitrary units. The labels refer to the *J*-values of the final level of the emission transition $^5D_0 \rightarrow {}^7F_J$. The inset shows an amplification of the region around 540 nm where weak transitions from the $^5D_1$ level could be detected.

unchanged, apart from the disappearance of the $^5D_1$ emission lines and a slight decrease in the emission intensity (viz. 10% upon 310 nm excitation). The lifetime of the $^5D_0$ level of the Eu^{3+} ion in $Eu(bpyO_2)_4(ClO_4)_3$ is 589 μs at 77 K, decreasing to 540 μs at 298 K.

The excitation spectrum of the emission of $Eu(bpyO_2)_4(ClO_4)_3$ at 4.2 K is shown in Fig. 4, consisting of two broad bands in the UV region, with maxima at 310 nm and 360 nm, and 4f–4f excitation lines. The intensity of the band at 310 nm is about four times that of the band at 360 nm. The excitation spectrum at room temperature shows the same features, but the thermal quenching is stronger for the band at 360 nm, which has its intensity decreased by 40%, whereas the band at 310 nm decreases by only 10%. Furthermore, the latter band broadens and

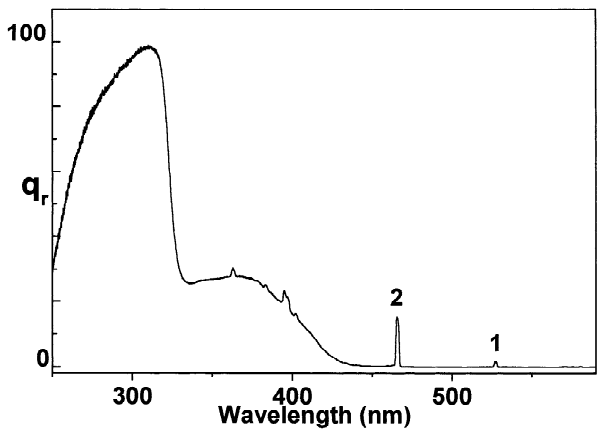

Fig. 4. The excitation spectrum of the $^5D_0$ emission ($\lambda_{em} = 611.4$ nm) of Eu^{3+} in $Eu(bpyO_2)_4(ClO_4)_3$ at 4.2 K. The labels refer to the *J*-values of the final level of the excitation transitions $^7F_0 \rightarrow {}^5D_J$ of the Eu^{3+} ion. q_r gives the relative quantum output.

shifts its maximum to 315 nm. The room temperature quantum yield of the Eu^{3+} emission is 15% upon excitation at 365 nm.

3. Theoretical analysis

The luminescence quantum yield depends on a balance between absorption and radiative and nonradiative rates in the compound, including intramolecular energy transfer rates. This balance is usually treated by a set of rate equations, which describe the time evolution of the populations of the energy levels involved in the luminescence process [1]. The rate equation for a given level, say *p*, has the general form:

$$\frac{d\eta_p}{dt} = -\left(\sum_i P_{ip}\right)\eta_p + \sum_j P_{pj}\eta_j \tag{2}$$

where P_{ip} represents a transition or transfer rate starting from state $|p\rangle$ and P_{pj} represents a transition or transfer rate ending up in this state. The ηs stand for the normalized populations of the states involved and in the steady state regime all $d\eta/dt$ are equal to zero. The system of rate equations given by Eq. (2) can be solved either analytically or numerically under the condition $\Sigma\eta_p = 1$. A procedure for numerical solutions by using the 4th order Runge–Kutta method has proven to be quite useful [15].

For the case of the compound studied here an appropriate energy level diagram is shown in Fig. 5.

The necessary matrix elements involving the ligand wave functions for the calculation of the energy transfer rates were obtained from the sparkle model [6] by using the crystallographic data presented in Section 2. The transfer rate for each channel indicated in Fig. 5 was then calculated on the basis of the theory developed in [7,8]. For the dipole–dipole, dipole–2^λ pole ($\lambda = 2$, 4 and 6) and exchange mechanisms we have the following expressions, respectively, for the transfer rate W_{ET}:

$$W_{ET} = \frac{2\pi}{\hbar}\frac{e^2 S_L}{(2J+1)GR_L^6} F \sum_{\lambda=2,4,6} \Omega_\lambda^{e.d.} \left\langle \alpha' J' \| U^{(\lambda)} \| \alpha J \right\rangle^2 \tag{3}$$

$$W_{ET} = \frac{2\pi}{\hbar}\frac{e^2 S_L}{(2J+1)G} F \sum_{\lambda=2,4,6} \gamma_\lambda \left\langle \alpha' J' \| U^{(\lambda)} \| \alpha J \right\rangle^2 \tag{4}$$

and

$$W_{ET} = \frac{8\pi}{3\hbar}\frac{e^2(1-\sigma_0)^2}{(2J+1)R_L^4} F \left\langle \alpha' J' \| S \| \alpha J \right\rangle^2 \sum_m \left| \left\langle \phi \left| \sum_k \mu_z(k) s_m(k) \right| \phi' \right\rangle \right|^2 \tag{5}$$

where the energy mismatch factor, *F*, has been given by the following approximate expression:

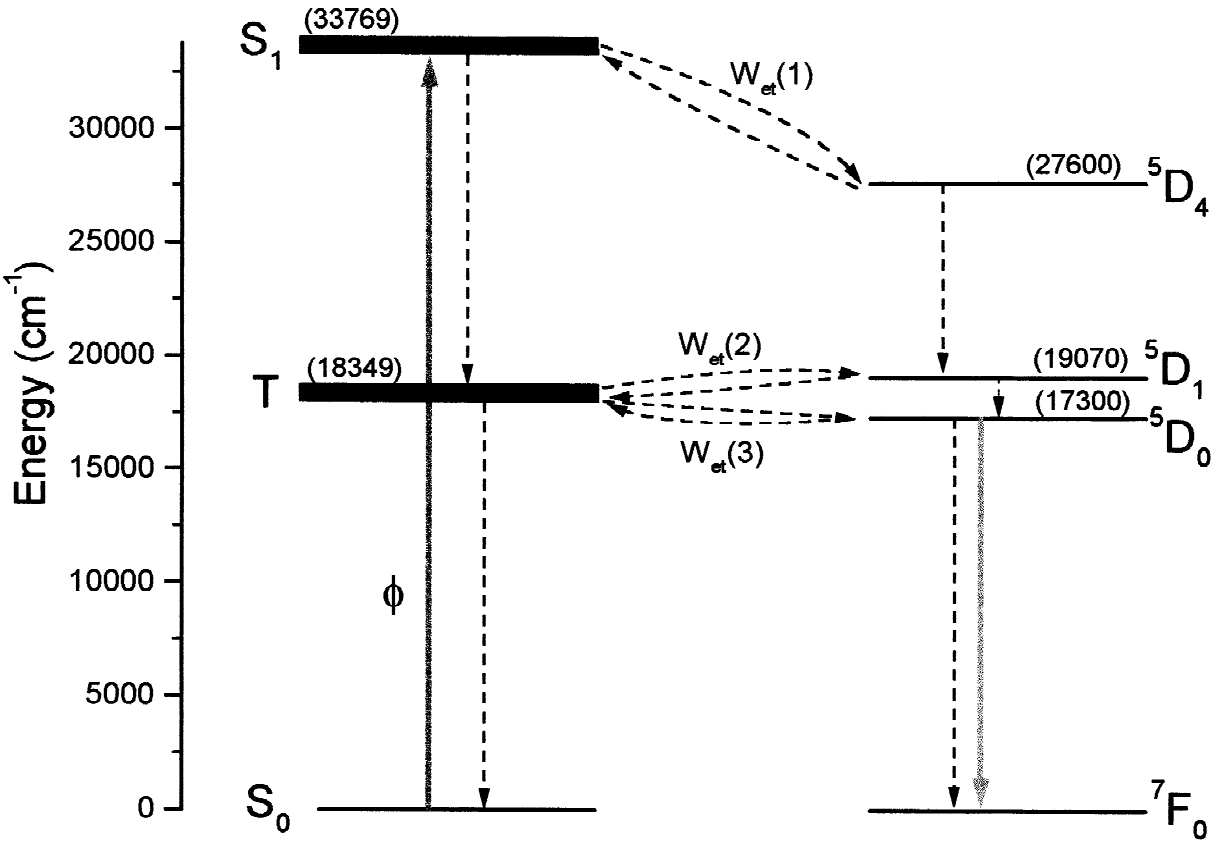

Fig. 5. Energy levels diagram showing the energy transfer channels used in the present analysis of the quantum yield of the luminescence in the complex $Eu(bpyO_2)_4(ClO_4)_3$.

$$F = \frac{1}{\hbar\gamma_L}\sqrt{\frac{\ln 2}{\pi}}\exp\left[-\left(\frac{\Delta}{\hbar\gamma_L}\right)^2 \ln 2\right] \quad (6)$$

where γ_L is the ligand state band width at half-height and Δ is the difference between the donor and acceptor transition energies involved in the transfer process. In Eqs. (3) and (4) S_L is the dipole strength associated with the transition $\phi \rightarrow \phi'$ in the ligand and G is the degeneracy of the corresponding initial state. The quantities $\langle \alpha' J' \| U^{(\lambda)} \| \alpha J \rangle$ are reduced matrix elements of the unit tensor operators $U^{(\lambda)}$, between the initial (αJ) and final ($\alpha' J'$) manifolds of the lanthanide ion. The $\Omega_\lambda^{e.d.}$s correspond to the forced electric dipole contribution to the so-called intensity parameters of 4f–4f transitions and the quantities γ_λ are given by:

$$\gamma_\lambda = (\lambda + 1)\frac{\langle r^\lambda \rangle^2}{(R_L^{\lambda+2})^2}\langle 3\|C^{(\lambda)}\|3\rangle^2 (1 - \sigma_\lambda)^2 \quad (7)$$

where $\langle r^\lambda \rangle$ is the radial expectation value of r^λ for 4f electrons, $\langle 3\|C^{(\lambda)}\|3\rangle$ is a reduced matrix element of the Racah tensor operator $C^{(\lambda)}$ and the σ_λs are screening factors due to the filled 5s and 5p sub-shells of the lanthanide ion [1]. In Eq. (5) S is the total spin operator (in units of $\hbar$) of the lanthanide ion, μ_z is the z component of the dipole operator and s_m is a spherical component of the spin operator both for the ligand electrons. The screening factor σ_0 is of the same nature as those appearing in Eq. (7) (with λ equal to zero). R_L is the distance from the lanthanide ion to the region of the ligand molecule in which the ligand donor (or acceptor) state is localized.

The radiative transition rates from the emitting level $^5D_0$ were calculated from the well-known theory of 4f–4f intensities [16], according to the procedure described in [1,17]. Firstly, from the crystallographic data we have performed a calculation of ligand field parameters, both of even and odd ranks, and then we have proceeded with the calculation of the forced electric dipole contribution to the intensity parameters ($\Omega_\lambda^{e.d.}$), which are necessary to the evaluation of the energy transfer rates by the multipolar mechanism. An effective nonradiative decay rate, towards the $^5D_0$ level, equal to 10^6 s^{-1} was assumed; a value which is based on the risetime of this level in a coordination compound [1]. An approximate nonradiative decay component from this level was obtained from the difference between the inverse of its lifetime and its total radiative decay rate, without considering the forward and back-transfer rates involved. From the ligand side the values of the nonradiative rates for intersystem crossing were assumed to be of the same order as those that have been previously optimized for compounds with β-diketo-

nate ligands [1,15]: $\sim 10^8$ s^{-1}, for the $S_1 \rightarrow T$ decay, and $\sim 5 \times 10^5$ s^{-1} for the $T \rightarrow S_0$ decay.

The theoretical luminescence quantum yield is given by [1]:

$$q_{\text{theo}} = \frac{\eta(^5D_0)}{\phi\eta(S_0)\tau(^5D_0)} \quad (8)$$

Here ϕ is the photon absorption rate by the ligand, from state $|S_0\rangle$ to state $|S_1\rangle$, and $\tau(^5D_0)$ is the radiative lifetime of the $^5D_0$ level.

4. Discussion

The focus of the present work is the emission quantum yield. Following the procedure described in Section 3 we have calculated, from Eq. (8), a q-value equal to 19.6%, which is in good agreement with experiment (15%). This rather low q-value cannot be explained in terms of a particularly important nonradiative decay channel from the $^5D_0$ level, due to coupling with a localized vibrational mode, since no significant variation of the $^5D_0$ lifetime with temperature, from 77 K to 298 K, was detected. Also, it cannot be explained in terms of the total radiative decay rate from this level, since the present value of this quantity (984 s^{-1}) is comparable with those found in compounds with β-diketones ligands. Since our experimental data show no evidence of the existence of LMCT states in the spectral region studied, the analysis points to the relative energy position of the ligand triplet level (18,394 cm^{-1}) with respect to the $^5D_1$ (19,070 cm^{-1}) and $^5D_0$ (17,300 cm^{-1}) states of the Eu^{3+} ion.

As in the cases of previous similar analyses [1,15], we have noticed that the energy transfer pathway involving the ligand singlet state S_1 has practically no influence on the q-value. The fact that the triplet level lies ~ 700 cm^{-1} below the $^5D_1$ manifold leads to a $^5D_1 \rightarrow T$ back-transfer rate which is higher than the corresponding forward rate by a factor of approximately 30, both rates being largely dominated by the exchange mechanism. For the $^5D_0$ level the forward transfer rate is higher than the corresponding back-transfer rate by more than two orders of magnitude. However, curiously enough, this is not sufficient to compensate for the reverse situation that is found for the $^5D_1$ manifold, and the overall balance between rates leads to a low q-value. This is certainly connected with the fact that the $^5D_1 \rightarrow T$ back-transfer rate is very high. It is higher than the forward transfer rate to the $^5D_0$ level by a factor of 3.5. These transfer rate values are presented in Table 2.

A question may be raised on the influence of the *N*-oxide groups on the energy position of the ligand triplet state. The emission spectrum of isolated bipyridine in solid state at 77 K shows an emission band peaked at 390 nm, which is assigned to the $S_1 \rightarrow S_0$ fluorescence, and a band peaked at 540 nm which is assigned to the $T \rightarrow S_0$ phosphorescence [18]. This latter band coincides, in shape and position, with the triplet emission observed in the $Lu(bpyO_2)_4(ClO_4)_3$ compound (Fig. 2). Thus, no influence of the *N*-oxide groups on the triplet state seem to occur, though these groups lead to a higher chemical stability, in comparison with the bpy ligand, due to their donor characteristics. An interesting and relevant fact is that we have also performed a calculation of the q-value by decreasing the energy of the triplet state and have found that a slight decrease in this energy, by say 500 cm^{-1}, is sufficient to quench the Eu^{3+} luminescence almost completely. This fact might suggest the compound here studied as a sensor for pressure [15]. On the other hand, derivatives of the bpy ligand bearing groups that raise the triplet energy are expected to increase the emission quantum yield.

Acknowledgements

The authors acknowledge the CNPq, PADCT and FACEPE (brazilian agencies) for financial support. They are grateful to Dr S. Alves Jr. (UFPE — Brazil) for providing the spectral data on the bipyridine ligand and to Prof. A. Meijerink (UU — The Netherlands) for kindly allowing the use of his laboratory facilities. This work was partially supported by the Foundation for Polish Science (grant MOLTEK'96) and by KBN.

References

[1] G.F. de Sá, O.L. Malta, C. de Mello Donegá, A.M. Simas, R.L. Longo, P.A. Santa-Cruz, E.F. da Silva Jr., Coord. Chem. Rev. 196 (2000) 165.
[2] E. Huskowska, J.P. Riehl, J. Lumin. 86 (2000) 137, and refs therein.
[3] P. Gawryszewska, M. Pietraszkiewicz, J.P. Riehl, J. Legendziewicz, J. Alloys Comp. 300 (2000) 283.
[4] P. Gawryszewska, L. Jerzykiewicz, M. Pietraszkiewicz, J. Legendziewicz, J.P. Riehl, Inorg. Chem. (in press).

Table 2
Comparison between theoretical and experimental values of the emission quantum yield. A_{RAD} is the total spontaneous radiative decay rate from the $^5D_0$ level. $W_{ET}(3)$ and $W_{ET}(2)$ are indicated in Fig. 5

A_{RAD}	$W_{ET}(3)$ (s^{-1})		$W_{ET}(2)$ (s^{-1})		q (%)	
(s^{-1})	Transfer	Back transfer	Transfer	Back transfer	EXP	THEOR
984.5	6.8×10^8	4.3×10^6	2.4×10^9	$7.4 \cdot 10^7$	15.0	19.6

[5] L. Prodi, M. Maestro, V. Balzani, J.-M. Lehn, C. Roth, Chem. Phys. Lett. 180 (1991) 45.
[6] A.V.M. de Andrade, N.B. da Costa Jr., A.M. Simas, G.F. de Sá, Chem. Phys. Lett. 227 (1994) 349.
[7] O.L. Malta, J. Lumin. 71 (1997) 229.
[8] F.R.G. e Silva, O.L. Malta, J. Alloys Comp. 250 (1997) 427.
[9] E. Huskowska, J. Legendziewicz, J.P. Riehl, (to be published).
[10] Kuma KM4CCD Software, version 161, Kuma Diffraction (1999) Wrocław, Poland.
[11] G.M. Sheldrick, Acta Crystallogr. A46 (1990) 467.
[12] G.M. Sheldrick, SHELXL93. Program for the Refinement of Crystal Structures, University of Göttingen, Germany, 1993.
[13] A.R. Al-Karaghouli, R.O. Day, J.S. Wood, Inorg. Chem. 17 (1978) 3702.
[14] C.D. Paul-Roth, J.-M. Lehn, J. Guilhem, C. Pascard, Helv. Chim. Acta 78 (1995) 1895.
[15] O.L. Malta, F.R.G. e Silva, R. Longo, Chem. Phys. Lett. 307 (1999) 518.
[16] C. Görller-Walrand, K. Binnermans, in: K.A. Gshneider Jr., L. Eyring (Eds.), Hand Book on the Physics and Chemistry of the Rare Earths, Vol. 25, North–Holland, 1998, p. 101, Chapter 167.
[17] O.L. Malta, M.A. Couto dos Santos, L.C. Thompson, N.K. Ito, J. Lumin. 69 (1996) 77.
[18] S. Alves, Jr., Private communication.